

## Cu Induced Optical Transitions in MOCVD Grown Cu Doped GaN

Jayantha Senawiratne<sup>1</sup>, Martin Strassburg<sup>1,2</sup>, Adam Payne<sup>2</sup>, Ali Asghar<sup>2</sup>, William Fenwick<sup>2</sup>, Nola Li<sup>2</sup>, Ian Ferguson<sup>2</sup>, and Nikolaus Dietz<sup>1,\*</sup>

<sup>1</sup>Georgia State University, Department of Physics and Astronomy, Atlanta, GA 30303-4106, U.S.A.

<sup>2</sup>Georgia Institute of Technology, School of Electrical and Computer Engineering, Atlanta, GA 30322-0250, U.S.A.

### ABSTRACTS

Optical and structural properties of *in situ* Cu doped GaN thin films grown on sapphire substrates were optically investigated by means of Raman, photoluminescence (PL), and absorption spectroscopy. Different Cu concentrations in the films were analyzed by secondary ion mass spectroscopy (SIMS) and found to vary from  $2 \times 10^{16} \text{ cm}^{-3}$  to  $5 \times 10^{17} \text{ cm}^{-3}$ . Raman studies confirmed high crystalline quality of GaN:Cu with no major structural damages due to Cu incorporation. PL investigation revealed that the origin of the emission around 2.4 eV is most likely due to Cu incorporation. The electrical conductivity of the samples was analyzed by Hall measurements and the found semi-insulating behavior was assigned to the compensation of intrinsic donors by the deep Cu acceptor states.

### INTRODUCTION

Copper incorporated in GaN on lattice sites acts as double acceptor and has therefore attracted increasing attention in the recent years. High-Ohmic material can be fabricated because of the deep acceptor-like states introduced by Cu that compensate residual donors [1]. Using Coulomb pairing, Cu was applied for co-doping purposes that have been applied to create shallow acceptor complexes [2]. Furthermore, copper electronic properties as a transition metal renders it as a candidate for spintronics material.

The Cu dopants can be introduced into GaN during the growth or by ion implantation. Ion implantation has become more popular, because it is a more controlled and a precise method of doping a selective area of the sample. However, crystalline damage during the ion implantation is unavoidable, since it is a thermodynamically unstable method [3,4]. Therefore, application of *in situ* doping of Cu has an advantage since this process does not introduce damage to the lattice structure.

This work reports on the *in situ* incorporation of Cu in metal organic chemical vapor deposition (MOCVD) grown GaN. In addition to that, structural and Cu induced optical transitions were investigated by different means of optical spectroscopy.

### EXPERIMENTAL DETAILS

Cu doped GaN layers on sapphire substrates were grown by metal organic chemical vapor deposition (MOCVD), using ammonia and trimethyl gallium (TMGa) as nitrogen and gallium sources, respectively. In addition, different Cu concentrations in the layers were introduced

---

\* Corresponding author: ndietz@gsu.edu

during the growth by varying the flow of the Cu source, (N,N'-Diisopropylacetamidinato) copper(I), to the reactor. The precursors were transferred to the reactor using hydrogen gas flow.

The stoichiometric analysis of the Cu concentration in the films were performed by secondary ion mass spectroscopy (SIMS) and revealed Cu concentrations of sample A, B, C, and D as high as  $2 \times 10^{16} \text{ cm}^{-3}$ ,  $4 \times 10^{16} \text{ cm}^{-3}$ ,  $2 \times 10^{17} \text{ cm}^{-3}$ , and  $5 \times 10^{17} \text{ cm}^{-3}$ , respectively. Besides, homogenous distribution of Cu in the film was confirmed by SIMS depth profile. Furthermore, from XRD experiment, growth of hexagonal GaN:Cu has been confirmed.

Optical investigation of GaN:Cu epilayers were performed using Raman, PL, and absorption spectroscopy. The Raman spectroscopy was performed in a backscattering geometry using a Renishaw RM series Raman spectrometer and a custom built Raman spectrometer. The latter consists of a McPherson triple grating monochromator system connected to liquid nitrogen cooled charged couple device (CCD) detector. The PL and transmission measurements of the thin films were performed using a single grating monochromator with a focal length 0.2 m that connected to the photomultiplier detector (Hamamatsu R 928). The second harmonic generation of a Ti:sapphire laser at an energy 3.49 eV was used as the PL excitation source. Deuterium and halogen lamp were employed as light sources for the transmission measurements.

## RESULTS AND DISCUSSION

The Cu induced structural properties of GaN:Cu thin films were investigated by Raman spectroscopy. The hexagonal wurtzite structure of GaN belongs to the  $C_{6v}^4$  space group symmetry with two Ga-N pairs in the primitive unit cell. According to predictions of group theory analysis, at the zone center ( $k = 0$ ), following Raman-active phonon modes [5] exists for the wurtzite symmetry:  $A_1 + E_1 + E_2(\text{low}) + E_2(\text{high})$ . Of which,  $A_1$  and  $E_1$  modes polarize into longitudinal (LO) and transverse (TO) components. According to the Raman selection rules, different Raman modes can be observed at different scattering configurations. The present Raman study was performed in a backscattering geometry choosing z-axis along (0001) direction at backscattering configuration *i.e.*, at  $z(.,.)z$ . At this scattering configuration, only  $A_1(\text{LO})$ ,  $E_2(\text{high})$  and  $E_2(\text{low})$  modes are allowed by the Raman selection rules.

As shown in figure 1, the Raman spectra of GaN:Cu is dominated by the symmetry-allowed  $E_2(\text{high})$  and  $A_1(\text{LO})$  modes. In addition, symmetry-forbidden,  $A_1(\text{TO})$ ,  $E_1(\text{TO})$ , and  $E_1(\text{LO})$  modes were observed with very low intensity. Raman modes from the sapphire substrate were also detected at  $576 \text{ cm}^{-1}$  and  $750 \text{ cm}^{-1}$  due to the high penetration depth of the laser at wavelength well below the GaN bandgap energy. Furthermore, a new Raman mode was observed around  $711 \text{ cm}^{-1}$ . Lorentzian curve fitting was applied to determine the exact energies of the respective Raman modes. In figure 3, the Lorentzian fit for sample #D is exemplarily given. According to the fitting results,  $E_2(\text{high})$  mode was found to be dominated in the spectra of each sample in the range  $567\text{-}569 \text{ cm}^{-1}$ . Its small full width half maximum (FWHM) of less than  $3.3 \text{ cm}^{-1}$  indicates high crystalline quality. Besides,  $A_1(\text{LO})$  mode was observed at  $\sim 734 \text{ cm}^{-1}$ . The FWHM of this mode was slightly increased with increasing Cu concentration (see table I). According to the Hall measurements, free carrier concentration is significantly low in all studied samples, hence, contribution from the plasmons-phonon interaction for the broadening of  $A_1(\text{LO})$  structure is insignificant. As Popovici *et al.* [6] predicted, in addition to the free-carrier mediated plasmon-phonon interaction, lattice imperfections also introduces the broadening of  $A_1(\text{LO})$  structure. Therefore, the possible culprit of broadening of  $A_1(\text{LO})$  was assigned due to minor lattice imperfections due to Cu incorporation.

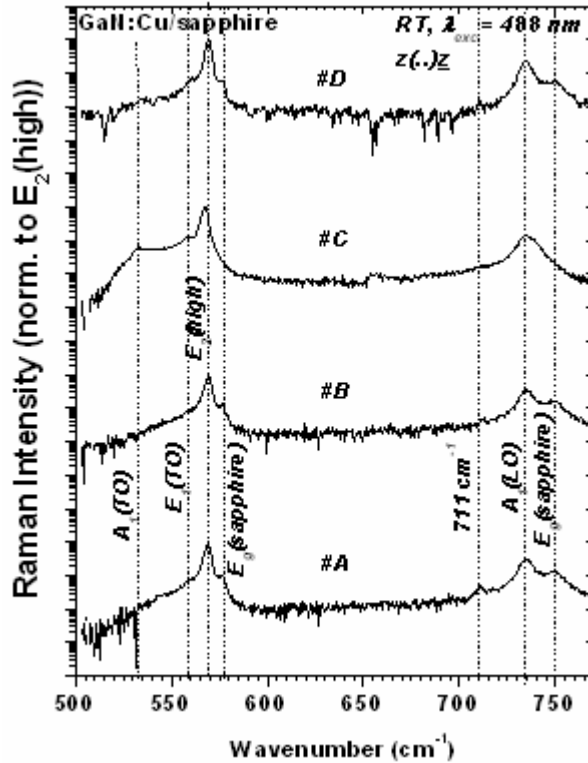


**Figure 1.** Room temperature Raman spectra of Cu doped GaN under backscattering geometry.

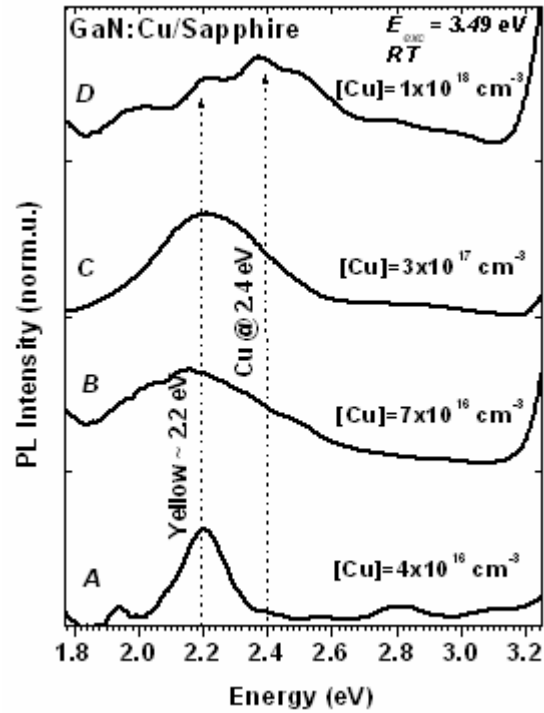


**Figure 2.** Room temperature PL spectra of Cu doped GaN for different Cu concentration. The emission at 2.4 eV increases with [Cu]

**Table I.** Raman peak position and FWHM of different Raman modes observed by Lorentzian fitting.

Sample ID	A <sub>1</sub> (TO) in cm <sup>-1</sup>		E <sub>1</sub> (TO) in cm <sup>-1</sup>		E <sub>2</sub> (high) in cm <sup>-1</sup>		A <sub>1</sub> (LO) in cm <sup>-1</sup>		E <sub>1</sub> (LO) in cm <sup>-1</sup>	
	Position	FWHM	Position	FWHM	Position	FWHM	Position	FWHM	Position	FWHM
A	533.7	17.5	559.8	15.0	568.9	3.1	734.5	7.1	739.7	11.0
B	533.7	17.5	559.1	15.0	569.2	3.2	734.7	7.6	741	13.2
C	534.6	17.6	558.6	12.2	567.3	3.2	734.5	8.9	739.7	6.4
D	534.6	9.2	559.9	2.6	569.3	2.6	734.5	9.4	739	12.1

In addition to the Raman modes described above, symmetry-forbidden A<sub>1</sub>(TO), E<sub>1</sub>(TO), and E<sub>1</sub>(LO) modes, at z(.,.)z scattering configuration, were observed at ~ 533 cm<sup>-1</sup>, 559 cm<sup>-1</sup>, 740 cm<sup>-1</sup>, respectively. The intensities of forbidden modes are extremely weak. Its existence is attributed either to lattice imperfections and/or to the non-perfect scattering geometry leading to relaxation of Raman selection rules as described above.

The Raman mode at 710 cm<sup>-1</sup> with slightly higher intensity was observed in sample A and B, while in sample C and D it was barely detectable due to its very low intensity. The appearance of this peak did also not show any relation to Cu incorporation. However, this mode was strongest in the thinnest sample, A. In addition, its intensity decreases with increasing the film thickness. Moreover, using a separate Raman experiment, it was observed that the intensity of

the Raman mode at  $\sim 710 \text{ cm}^{-1}$  significantly increases, when laser spot was focused on the substrate-epilayer interface.

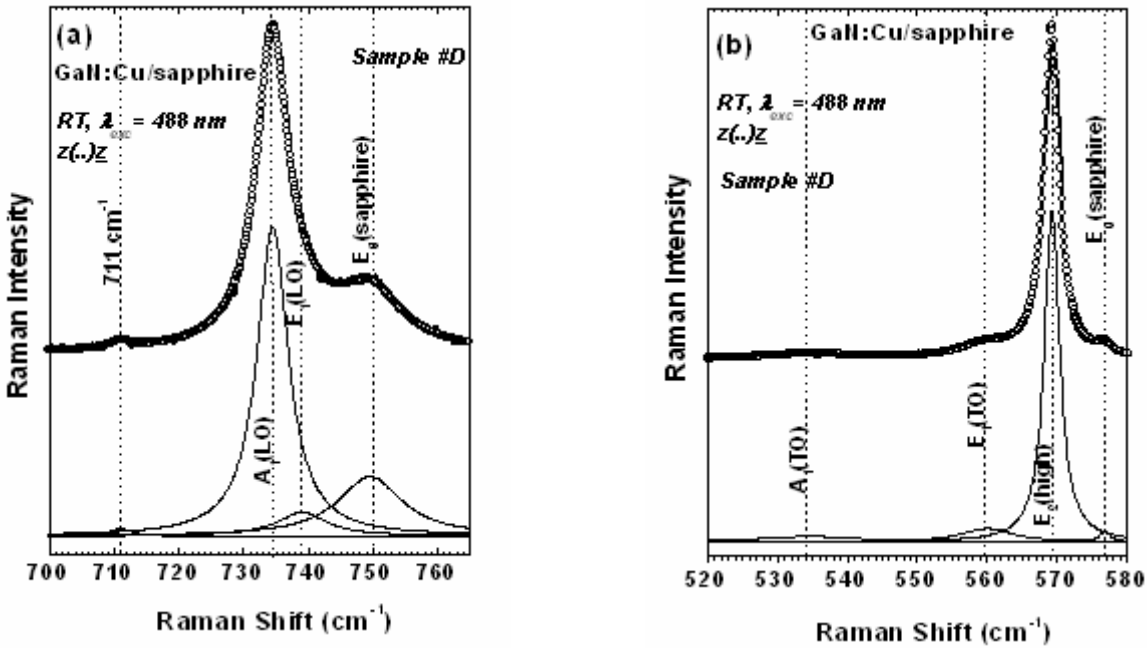


**Figure 3** (a) Raman spectrum of GaN:Cu/Sapphire (sample #D) and identification of different Raman modes using Lorentz fits, in the Raman scattering range (a) 700-765  $\text{cm}^{-1}$ , and (b) 520-580  $\text{cm}^{-1}$ . The top curve represents experimental Raman scattering with circles representing Lorentzian fitting curve, while the Lorentz curves due to the different modes are shown below.

In addition to the obtained structural properties, the static dielectric constant of GaN:Cu in parallel ( $\epsilon_{//0}$ ) and perpendicular ( $\epsilon_{\perp 0}$ ) directions were calculated by applying phonon frequencies to the Lyddane-Sachs-Teller relation [7]. In the infrared (IR) spectral region GaN is approximately isotropic [8]. Therefore, the optical dielectric constants along parallel and perpendicular directions are equal ( $\epsilon_{\perp\infty} = \epsilon_{//\infty}$ ). In our calculations, the optical dielectric constant of 5.29 [9] was used to determine the static dielectric constant. The results showed that the static dielectric constant of GaN:Cu to be  $\epsilon_{//0} \sim 10.0$  and  $\epsilon_{\perp 0} \sim 9.2$ . These values are in good agreement with those of previously reported static dielectric constants of GaN films [9], as expected since the Cu concentration of the samples under investigation is relatively low.

Fundamental absorption edge was detected at 3.44 eV by room temperature optical transmission spectroscopy (not shown here). Moreover, the PL spectroscopy was applied to investigate Cu induced electronic states in GaN:Cu. The results of PL measurement of GaN:Cu with different Cu concentrations is shown in figures 2. The PL spectra consist of broad emission band between 1.8 and 2.6 eV. Moreover, broad blue emission band at  $\sim 2.75 \text{ eV}$  has been observed with low intensity. The yellow luminescence band centered at  $\sim 2.2 \text{ eV}$  is significant in the spectrum of each sample. Also, an emerging green emission, in the shoulder of the yellow luminescence, at 2.4 eV was observed with increasing Cu concentration. In addition to that, a steep increase of PL intensity above 3.15 eV and below 1.8 eV has been observed due to background light of the first and second order of the excitation source.

According to the observed PL data, it can be concluded that the intensity of the green band at  $\sim 2.4$  eV is the lowest for the sample with the lowest Cu concentration (#A), while it is the highest for sample (#D) having a Cu concentration of  $5 \times 10^{17} \text{ cm}^{-3}$ . Furthermore, the intensity of the green emission at 2.4 eV seems to increase with increasing Cu concentration. According to Monteiro *et al.* [10], in Ca doped GaN, several overlapping PL bands have been observed in the range 1.8-2.95 eV, and in addition to that, an emission peak at 2.59 eV has been attributed to the Ca related defect-defect recombination between the deep donor and acceptor pair. Besides that, Korotkov *et al.* [11] reported on emerging green emission band in the range of 2.4-2.5 eV in Mg-doped GaN. Therefore, based on similar results of group II related defects and dominance of the green emission with respect to Cu concentration, it can be suggested that the origin of the green emission in the presented study is due the Cu induced optical transitions associated with deep Cu induced states.

Besides, the yellow emission band centered at  $\sim 2.2$  eV is visible in the PL spectra of each sample. According to the literature, the yellow luminescence originates by native defects such as Ga vacancies [12] and this emission band vanishes when introducing p-type doping [13], confirming its assignment to the Ga vacancy. In spite of that, the yellow band persists when sample remains n-type or semi-insulating [13,14,15]. Therefore, considering the semi-insulating electrical properties of the selected sample series, with no major change in the yellow PL upon Cu incorporation, it can be suggest that the origin of the yellow luminescence band is most likely due to the native defect like Ga vacancies.

The electrical conductivity of the sample series were observed by Hall method and revealed semi-insulating electrical behavior. According to the literature, from EPR investigations of Cu doped GaN it was found that Cu is observed in GaN as a deep acceptor state [16]. Hence, the activation probability of holes (inherent to the deep Cu-induced acceptor states) at room temperature results in a low electrical conductivity or semi-insulating behavior. Furthermore, it has been found that also shallow acceptors are strongly compensated when grown under H-rich ambient conditions, such as reported for e.g., MOCVD-grown Mg doped GaN [17,18]. With respect to the applied growth technique, the deep binding energy and the Cu concentration, compensation by residual donor states may mostly hold for the low electrical conductivity in Cu doped GaN.

## CONCLUSION

The MOCVD growth of *in situ* Cu-doped GaN was reported. The structural properties investigated by Raman studies confirmed high crystalline quality of GaN:Cu with minimum damage to the hexagonal lattice structure due to Cu incorporation. Moreover, the origin of the PL emission around 2.4 eV was assigned to Cu induced optical transitions associated with deep Cu states. Compensation of Cu acceptor states by residual donor like hydrogen and poor activation probability of deep of Cu states are responsible for the semi-insulating electrical conductivity.

## ACKNOWLEDGEMENTS

The growth GaN:Cu is performed at Georgia Tech is supported by DARPA's suvos program managed by John Carrano. M.S. gratefully acknowledges the support of the Alexander von Humboldt-foundation.

## REFERENCES

---

- 1 J. Senawiratne, M. Strassburg, A. M. Payne, A. Asghar, W. E. Fenwick, N. Li, M. Wagner, A. Hoffmann, N. Dietz, and I. T. Ferguson, submitted to Phys. Stat. Sol. (c) (2005).
- 2 Z.C. Feng, A.M. Payne, D. Nicol, P.D. Helm, I. Ferguson. J. Senawiratne, M. Strassburg, N. Dietz, Ch. Hums and A. Hoffman, in “GaN and related alloys 2003”, ed, H.M. Ng. M. Wraback, K. Hiramatsu, N. Grandjean; Mat. Res. Soc. Symp. Proc. **798**, pp. 545 -550 (2004).
- 3 W. Limmer, W. Ritter, R. Sauer, B. Mensching, C. Liu, and B. Rauschenbach, Appl. Phys. Lett **72**, 2589, (1998).
- 4 B. Boudart, Y. Guhel, J. C. Pesant, P. Dhamelincourt, and M.A. Poisson, J. Phys.: Condens. Matter **16**, 49 (2004).
- 5 C.A. Arguello, D. L. Rousseau, and S.P.S. Porto, Phys. Rev. **181**, 1351 (1969).
- 6 G. Popovici, G. Y. Xu, A. Botchkarev, W. Kim, H. Tang, A. Salvador, M. Morkoc, R. Strange, and J. O. White, J. Appl. Phys. **82**, 4020 (1997).
- 7 N. W. Ashcroft, N. D. Mermin: Solid State Physics (Holt, Rinehart and Winston, New York 1976).
- 8 D.D. Manchon, A. S. Barker, P. J. Dean, R. B. Zetterstrom: Solid State Commun. **8**, 1227 (1970).
- 9 T. Azuhata, T. Sota, K. Suzuki, S. Nakamura: J. Phys.: Condens. Matter **7**, L129 (1995).
- 10 T. Monteiro, C. Boemare, M. J. Soares, E. Alves, and C. Lie, Physica B, **308-310**, 42 (2001).
- 11 R. K. Korotkov, J. M. Gregie, and B. W. Wesseles, Amter. Res. Soc. Symp. Proc. 639, G 6.39 (2001).
- 12 J. Neugebauer, and C. G. Van de Walle, Appl. Phys. Lett. **69**, 503 (1996).
- 13 S. Nakamura and G. Fosol, *The Blue Laser Diode* (Springer, Berlin, 1998).
- 14 J. K. Sheu, Y. K. Su, G. C. Chi, B. J. Pong, C. Y. Chen, C. N. Huang, and W. C. Chen, J. Appl. Phys. **84**, 4590 (1998).
- 15 M. W. Bayer *et al.*, Appl. Phys. Lett. **74**, 3281 (1999).
- 16 C. Bozdog, K. H. Chow, G. D. Watkins, H. Sunakawa, N. Kuroda, and A. Usai, Phys. Rev. B **62**, 12923, (2000).
- 17 A. Kaschner, H. Siegle, G. Kaczmarczyk, M. Strasbug, A. Hoffmann, C. Thomsen, U. Birkle, S. Einfeldt, and D. Hommel, Appl. Phys. Lett. **74**, 94720, (1999).
- 18 I. Nakamura, N. Iwasa, M. Senoh, and Mukai, Jpn. J. Appl. Phys., Part 1 **31**, 1258 (1992).